Adaptive hybrid predictive control for a combined cycle power plant optimization

D. Sáez[1, *, †], R. Zúñiga[1] and A. Cipriano[2]

[1]*Electrical Engineering Department, Facultad de Ciencias Físicas y Matemáticas, Universidad de Chile, Av. Tupper 2007, Santiago 837-0451, Chile*
[2]*Electrical Engineering Department, Facultad de Ingeniería, Pontificia Universidad Católica de Chile, Santiago, Chile*

SUMMARY

The design and development of an adaptive hybrid predictive controller for the optimization of a real combined cycle power plant (CCPP) are presented. The real plant is modeled as a hybrid system, i.e. logical conditions and dynamic behavior are used in one single modeling framework. Start modes, minimum up/down times and other logical features are represented using mixed integer equations, and dynamic behavior is represented using special linear models: adaptive fuzzy models. This approach allows the tackling of special non-linear characteristics, such as ambient temperature dependence on electrical power production (combined cycle) and gas exhaust temperature (gas turbine) properly to fit into a mixed integer dynamic (MLD) model. After defining the MLD model, an adaptive predictive control strategy is developed in order to economically optimize the operation of a real CCPP of the Central Interconnected System in Chile. The economic results obtained by simulation tests provide a 3% fuel consumption saving compared to conventional strategies at regulatory level. Copyright © 2007 John Wiley & Sons, Ltd.

KEY WORDS: supervisory control; hybrid predictive control; economic optimization; combined cycle power plant

1. INTRODUCTION

Combined cycle power plants (CCPPs) are part of the most common thermal power plant configuration. The usual configuration uses one gas turbine powered by some fossil fuel and produces

---

*Correspondence to: D. Sáez, Electrical Engineering Department, Facultad de Ciencias Físicas y Matemáticas, Universidad de Chile, Av. Tupper 2007, Santiago 837-0451, Chile.
†E-mail: dsaez@ing.uchile.cl

mechanical power *via* expansion of hot gases in the turbine. The steam turbine is powered by steam produced in a heat recovery steam generator (HRSG) that uses the still hot exhaust gases of the gas turbine to transform water into steam. This steam is also expanded in a turbine producing mechanical power. The mechanical power is transformed into electrical power using electrical generators.

The economic optimization of CCPP has been a matter of several research works in recent years. In [1], the CCPP is modeled using a mixed logical dynamical (MLD) framework considering start-up modes, on/off signals and turbine dynamics, and the optimization procedure maximizes the process earnings by choosing the optimum input signals. However, this approach does not consider fast dynamics of the control system. In [2], a complete model of a thermal unit is developed using integer variables to describe ramp constraints, start up procedures and minimum up/down time constraints. In [3], the integer variables related to model start up and shut down ramps are used for optimizing the economical dispatch and the optimal trajectories of start up and shut down. All these works optimize the hourly operation given by the economic dispatch; however, between two consecutive hours, the calculated controller outputs remain constant despite the fact that many conditions change, leading to suboptimal operation.

To tackle the real-time optimization of a CCPP in [4, 5] an optimizing supervisory algorithm based on predictive control is used, and in [6] predictive control is used on gasification units employing linearized neuronal models. In all these examples the CCPP operation is optimized in an economical way, but the prediction models do not consider the start up and shut down procedures or any other logic condition. The effect of ambient temperature and the relation between the thermodynamic efficiency and environmental conditions are not considered.

In this work, the CCPP is modeled as a hybrid system and apart from the start up and shut down procedures; the control system actions and the ambient temperature effect over the turbine efficiency are incorporated. Therefore, the controller is able to adapt itself to the ambient conditions. For representing the logical conditions and the dynamics together, we use MLD models, and for recasting the economic optimization as a control problem, an adaptive hybrid predictive control (AHPC) is used.

2. ADAPTIVE HYBRID PREDICTIVE CONTROL

The strategy of AHPC is based on the theory of model predictive control (MPC) [7] as well as the hybrid systems. The MPC controller determines a sequence of future control actions that minimizes a suitable objective function considering process constraints and using a prediction of the future controlled variables for a given prediction horizon.

In this work, MLD representations are considered because of their simplicity and flexibility for incorporation into MPC control algorithms. The next sections give a brief description of these schemes.

2.1. MLD modeling

The main idea of MLD modeling is to transform the hybrid features such as logical conditions into mixed integer inequalities [8]. This can be achieved using binary variables related to the truth

value of a logical sentence. The general MLD form of a hybrid system is

$$x(k+1) = Ax(k) + B_1 u(k) + B_2 \delta(k) + B_3 z(k)$$
$$y(k) = Cx(k) + D_1 u(k) + D_2 \delta(k) + D_3 z(k) \tag{1}$$
$$E_2 \delta(k) \leqslant E_3 z(k) + E_1 u(k) + E_4 x(k) + E_5$$

where $x = [x_c^T, x_l^T]^T \in R^{n_c} \times \{0, 1\}^{n_l}$ are the continuous and binary states, $u = [u_c^T, u_l^T]^T \in R^{m_c} \times \{0, 1\}^{m_l}$ are the inputs, $y = [y_c^T, y_l^T]^T \in R^{p_c} \times \{0, 1\}^{p_l}$ the outputs, and $\delta(k) \in \{0, 1\}^{\eta}$, $z(k) \in R^{r_c}$ represent the binary and continuous auxiliary variables, respectively. The constraints over state, input, $z(k)$ and $\delta(k)$ variables are included in the third term of Equation (1).

Generally, $\delta(k)$ is related to the truth value of a logical sentence or a binary input/output, and $z(k)$ is an auxiliary variable representing the multiplication between a real function and a binary variable.

2.2. Fuzzy modeling

In this work, the use of fuzzy modeling allows the representation of the non-linear behavior of a process by using smoother transitions between regions. The most used model for fuzzy modeling corresponds to the Takagi and Sugeno (T–S) fuzzy model [9]

$$\text{if } p^1(k) \text{ is } C_1^r \text{ and } \dots \text{ and } p^m(k) \text{ is } C_m^r \text{ then } A_r(z^{-1})y_r(k) = B_r(z^{-1})u(k-1) \tag{2}$$

where z^{-1} is the backward shift operator, $p(k) = (p^1(k), \dots, p^m(k))$ are fuzzy model inputs, C_i^r is the fuzzy set of variable i of rule r, $A_r(z^{-1})$ and $B_r(z^{-1})$ are the corresponding polynomials associated with the linear model of each rule r, and $y_r(k)$ is the output of rule r.

2.3. Adaptive fuzzy modeling

It is possible to derive from a T–S fuzzy model linear approximations that can be incorporated into the MLD scheme. This procedure consists of calculating the activation values for every rule using the current model input measurements and then the parameters of a current linear model are obtained using the evaluated activation degrees.

In this work, we exploit the structure of the fuzzy models used for representing the dynamics of a particular model where the activation values are functions of variables (p) which do not belong to the space state representation. If the activation value of the rule r is $\overline{w}_r = \overline{w}_r(p(k))$, the product being obtained from the membership grades involved in the same rule, then the final output becomes [9]

$$\overline{A}(z^{-1})y(k) = \overline{B}(z^{-1})u(k-1) \tag{3}$$

with

$$\overline{A}(z^{-1}) = \sum_{i=1}^{Nr} \overline{w}_i A_i(z^{-1}), \quad \overline{B}(z^{-1}) = \sum_{i=1}^{Nr} \overline{w}_i B_i(z^{-1})$$

where Nr is the number of rule.

This fuzzy approach corresponds to an adaptive linear model with time-variant coefficients and can be easily incorporated into MLD modeling framework.

2.4. Adaptive hybrid predictive control algorithm

In this work, the proposed control algorithm is based on MLD systems with an objective function given by the following general representation [8]:

$$
\min_{u_k^{k+N-1}} J(u_k^{k+N-1}, x(k)) = \sum_{j=0}^{N} \|u(k+j-1)-u_e\|_{Q_1}^2 + \|\delta(k+j)-\delta_e\|_{Q_2}^2 + \|z(k+j)-z_e\|_{Q_3}^2
$$

$$
+ \|x(k+j)-x_e\|_{Q_4}^2 + \|y(k+j)-y_e\|_{Q_5}^2 \tag{4}
$$

where k is the current time, $Q_1, \ldots, Q_5$ the weight matrixes, $x(k)$ the current state, (x_e, u_e) an equilibrium pair or a reference trajectory value, y_e the output reference value and N the prediction horizon. The optimal control sequence $u_k^{k+N-1} = (u(k) \ldots u(k+N-1))$ moves the state from $x(k)$ to x_e and minimizing the cost function (4) subject to (1) with $u(k)$ constant for $k \geqslant N_u$. N_u is the control horizon and δ_e, z_e are the auxiliary variables equilibrium point of the reference trajectory. The optimization procedure of (4) leads to mixed integer quadratic programming problems where the optimization vector is $(u(k), \ldots, u(t+N-1), \delta(k), \ldots, \delta(k+N-1), z(k), \ldots, z(k+N-1))$.

3. COMBINED CYCLE POWER PLANT MODELING

In this work, the CCPP will be modeled as a MLD system, considering the logical operational conditions, the dynamics of gas and steam turbines, continuous operational constraints and conventional control systems; the effect of ambient temperature is also incorporated. For the modeling of the ambient temperature, fuzzy T–S models are considered in order to capture its non-linear behavior over the power production. However, we propose to consider a linearized adaptive version of fuzzy models in order to use the MLD system representation that can be incorporated into the AHPC strategy as explained in Section 4.

3.1. Plant description

The main units of a CCPP are [10] a gas turbine, a HRSG and a steam turbine. Basically, the gas turbine consists of a compressor, a combustion chamber and the turbine itself. The air from the environment gets into the compressor to increase its pressure. Then, this compressed air gets into the combustion chamber where it is mixed with fuel; this mixture is burnt to increase the temperature of the air. Finally, the hot air is expanded in a turbine to generate mechanical power. The exhaust gases delivered by the gas turbine are used to warm water until it turns into steam. This task is performed by the HRSG, and the generated steam is used in a steam turbine to produce mechanical power. Both turbines use electrical generators to transform mechanical power to electrical power.

3.2. Regulatory control system

For the normal operation of the CCPP, the regulatory control system is the main control loop [10] where the control variables are the steam and gas turbine powers, frequencies and gas turbine exhaust temperature.
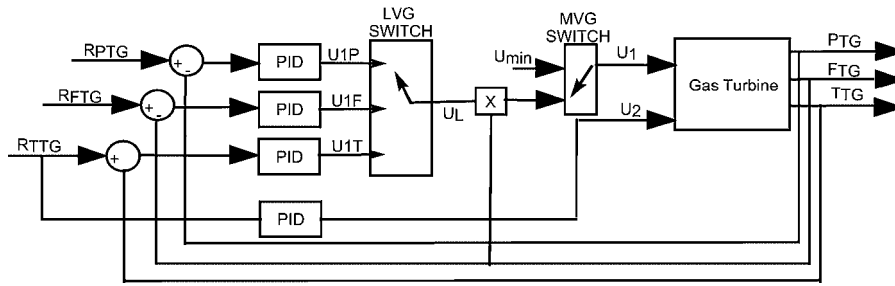
Figure 1. Standard gas turbine control system.

3.2.1. Gas turbine. Particularly, the main control variables for a gas turbine are the frequency, the electrical power and the exhaust gas temperature. The control loops consider switching PID controllers. Figure 1 shows a scheme of the control system used for a standard gas turbine where the main variables considered are:

- R_{PTG}, R_{FTG} and R_{TTG}: electrical power reference, electrical frequency reference and exhaust gas temperature reference, respectively.
- u_{1P}, u_{1F} and u_{1T}: fuel flow according to controller inputs, respectively.
- u_L: minimum between u_{1P}, u_{1F} and u_{1T}.
- u_{min}: minimum fuel flow.
- u_1: maximum between u_{min} and u_L.
- u_2: air flow to compressor.
- P_{TG}: electrical power.
- F_{TG}: electrical frequency.
- T_{TG}: exhaust gas temperature.

There are three PID controllers that calculate the required fuel flow based on the minimum value (u_L) among the output of the controllers for power, frequency and exhaust gas temperature. This value is multiplied by the frequency (u_{LF}) and enters the MVG block that selects the applied fuel flow (u_1) as the maximum value between the minimum fuel flow (u_{min}) and LVG output signal (u_{LF}) to maintain a stable flame. The last PID regulates the exhaust gas temperature by using the air flow entering the compressor (u_2).

In order to model this regulatory control system as MLD, it is necessary to make some simplifications [5]. The frequency signal is neglected in order to avoid the modeling of its complex non-linearity. This assumption is based on empirical experience from the real operation of combined cycle units.

3.2.2. Steam turbine. The steam turbine control system selects the steam flow to produce the desired mechanical power. The steam characteristics, such as pressure and temperature, are defined in the boiler which is an HRSG component. For this work we assume that the HSRG control system is good enough to provide these desired behaviors. The main variables for this control system are:

- R_{PTV}: electrical power reference for steam turbine.
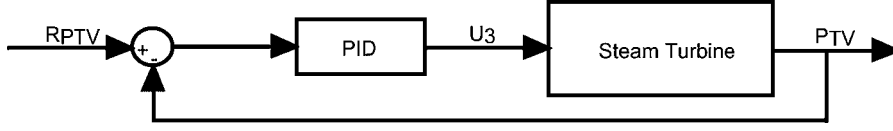- u_3: steam flow.
- P_{TV}: electrical power.

Figure 2. Standard steam control system.

Figure 2 shows the conventional steam turbine control system. The steam flow (u_3) is regulated by a PID controller according to the electrical power reference (R_{PTV}) and the actual electrical power (P_{TV}). It can be noticed that the steam flow strongly depends on the fuel and air flows in the gas turbine.

3.3. Dynamic process modeling

For incorporate the dynamic process, data from a CCPP are necessary in order to create an identification process. The auto-regressive model with exogenous variables (ARX) structure is used for the identification of the CCPP. The ARX model can be directly included in the MLD model. For the CCPP, the ARX models are

$$A_{TG1}(z^{-1})P_{TG}(k) = B_{TG1}(z^{-1})u_1(k) + B_{TG2}(z^{-1})u_2(k) + e_1(k)$$
$$A_{TG2}(z^{-1})T_{TG}(k) = B_{TG3}(z^{-1})u_1(k) + B_{TG4}(z^{-1})u_2(k) + e_2(k) \qquad (5)$$
$$A_{TV1}(z^{-1})P_{TV}(k) = B_{TV1}(z^{-1})u_1(k) + B_{TV2}(z^{-1})u_2(k) + B_{TV3}(z^{-1})u_3(k) + e_3(k)$$

where P_{TG} and T_{TG} are the electrical power and the exhaust gas temperature in the gas turbine, respectively, and P_{TV} is the electrical power in the steam turbine. u_1 is the fuel flow, u_2 the air flow and u_3 the steam flow. e_1, e_2, e_3 correspond to noise whites associated with unmeasured disturbances.

In this paper, since in Equation (5) the u_3 strongly depends on the fuel and air flows in the gas turbine, the inputs u_1 and u_2 will be neglected. Besides, this fact is more valid when the CCPP operates at base load. This behavior is based on the real data that show that the power produced by the steam turbine, P_{TV}, is mainly related to the steam flow, u_3, produced by the HRSG. Therefore, for ARX modeling of steam power, the polynomials $B_{TV1}(z^{-1})$ and $B_{TV2}(z^{-1})$ will be assumed to be equal to zero.

3.4. MLD modeling for regulatory level

As shown in Section 3.2, the control loop used for regulating the fuel flow is based on a switching strategy. According to the established assumptions, only the electrical power and the exhaust gas temperature are considered. Therefore, the following model for switching behavior is used:

$$\delta_{PT}(k) = 1 \ \Leftrightarrow \ u_{1P}(k) \leqslant u_{1T}(k)$$
$$u_1(k) = u_{1P}(k)\delta_{PT}(k) + u_{1T}(k)(1 - \delta_{PT}(k)) \qquad (6)$$
$$u_1(k) \geqslant u_{min}$$

The first and second statements in Equation (6), which represent the LVG block of Figure 1, use a binary variable $\delta_{\text{PT}}(k)$. The third inequality represents the MVG block. In order to obtain the MLD model, the mixed integer representation of Equation (6) is considered

$$M\delta_{\text{PT}}(k) \leqslant -(u_{1\text{P}}(k) - u_{1\text{T}}(k)) + M$$
$$(m - \varepsilon)\delta_{\text{PT}}(k) \leqslant (u_{1\text{P}}(k) - u_{1\text{T}}(k)) - \varepsilon \tag{7}$$
$$-u_1(k) \leqslant -u_{\min}$$

where M and m are the maximum and minimum values of $u_{1\text{P}}(k) - u_{1\text{T}}(k)$, respectively. ε is a small positive scalar.

The PID controllers are represented by the following discrete models:

$$u_{1\text{P}}(k) = u_{1\text{P}}(k-1) + (K_1 + I_1)(R_{\text{PTG}}(k) - P_{\text{TG}}(k)) - K_1(R_{\text{PTG}}(k-1) - P_{\text{TG}}(k-1))$$
$$u_{1\text{T}}(k) = u_{1\text{T}}(k-1) + (K_2 + I_2)(R_{\text{TTG}}(k) - T_{\text{TG}}(k)) - K_2(R_{\text{TTG}}(k-1) - T_{\text{TG}}(k-1)) \tag{8}$$
$$u_2(k) = u_2(k-1) + (K_3 + I_3)(R_{\text{TTG}}(k) - T_{\text{TG}}(k)) - K_3(R_{\text{TTG}}(k-1) - T_{\text{TG}}(k-1))$$

where K_1, I_1, K_2, I_2, K_3 and I_3 are the corresponding PID controller gains.

3.5. Logical condition modeling

The logical conditions of the CCPP operation will be modeled. The main logical conditions are related to 'on/off' commands and the delay between the 'on' command and the current electrical power production. The new variables introduced are:

- u_{l1}: binary variable related to the 'on/off' gas turbine command.
- u_{l2}: binary variable related to the 'on/off' steam turbine command.
- $\xi_{\text{on\_TG}}/\xi_{\text{on\_TV}}$: clock counter related to the consecutive time when the gas/steam turbines are producing electrical power.
- $\xi_{\text{off\_TG}}/\xi_{\text{off\_TV}}$: clock counter related to the consecutive time when the gas/steam turbines are not producing electrical power.
- $\xi_{\text{d\_TG}}/\xi_{\text{d\_TV}}$: clock counter related to the delay between the 'on' command and the actual electrical power production.
- $\delta_{\text{d\_TG}}/\delta_{\text{d\_TV}}$: binary variable related to delays.
- $\delta_{\text{on\_TG}}/\delta_{\text{on\_TV}}$: binary variable related to the electrical power production.

The following constraint related to the start up condition of the steam turbine power production is established in order to avoid the power production of the steam turbine if gas turbine is not already started up:

$$u_{l2} = 1 \implies u_{l1} = 1 \tag{9}$$

The mixed integer relation for Equation (9) is:

$$u_{l2} - u_{l1} \leqslant 1$$

The clock counter dynamics are governed by the following equations:

$$\xi_{\text{on\_TG}}(k + T_{\text{s}}) = (\xi_{\text{on\_TG}}(k) + T_{\text{s}})\delta_{\text{on\_TG}}(k)$$
$$\xi_{\text{on\_TV}}(k + T_{\text{s}}) = (\xi_{\text{on\_TV}}(k) + T_{\text{s}})\delta_{\text{on\_TV}}(k)$$
$$\xi_{\text{off\_TG}}(k + T_{\text{s}}) = (\xi_{\text{off\_TG}}(k) + T_{\text{s}})(1 - \delta_{\text{on\_TG}}(k))$$
$$\xi_{\text{off\_TV}}(k + T_{\text{s}}) = (\xi_{\text{off\_TV}}(k) + T_{\text{s}})(1 - \delta_{\text{on\_TV}}(k)) \tag{10}$$
$$\xi_{\text{d\_TG}}(k + T_{\text{s}}) = (\xi_{\text{d\_TG}}(k) - T_{\text{s}})u_{l1}(k) + D_{\text{TG}}(\xi_{\text{off\_TG}})(1 - u_{l1}(k))$$
$$\xi_{\text{d\_TV}}(k + T_{\text{s}}) = (\xi_{\text{d\_TV}}(k) - T_{\text{s}})u_{l2}(k) + D_{\text{TV}}(\xi_{\text{off\_TV}})(1 - u_{l2}(k))$$

where T_{s} is the sampling time. As an example of MLD modeling, the mixed integer relation for the first relation in Equation (10) is given by

$$-M_{\xi_{\text{on\_TG}}(k)+T_{\text{s}}}\delta_{\text{on\_TG}}(k) + z_{\text{on\_TG}}(k) \leqslant 0$$
$$m_{\xi_{\text{on\_TG}}(k)+T_{\text{s}}}\delta_{\text{on\_TG}}(k) - z_{\text{on\_TG}}(k) \leqslant 0$$
$$-m_{\xi_{\text{on\_TG}}(k)+T_{\text{s}}}\delta_{\text{on\_TG}}(k) + z_{\text{on\_TG}}(k) \leqslant (\xi_{\text{on\_TG}}(k) + T_{\text{s}}) - m_{\xi_{\text{on\_TG}}(k)+T_{\text{s}}}$$
$$M_{\xi_{\text{on\_TG}}(k)+T_{\text{s}}}\delta_{\text{on\_TG}}(k) - z_{\text{on\_TG}}(k) \leqslant -(\xi_{\text{on\_TG}}(k) + T_{\text{s}}) + M_{\xi_{\text{on\_TG}}(k)+T_{\text{s}}}$$

where $M_{\xi_{\text{on\_TG}}(k)+T_{\text{s}}}$ and $m_{\xi_{\text{on\_TG}}(k)+T_{\text{s}}}$ are the maximum and minimum values of $(\xi_{\text{on\_TG}}(k) + T_{\text{s}})$, respectively.

In the work, $D_{\text{TG}}(\xi_{\text{off\_TV}})$ corresponds to a delay which does not depend on the $\xi_{\text{off\_TG}}$ value, but the delay $D_{\text{TV}}(\xi_{\text{off\_TV}})$ is a function of $\xi_{\text{off\_TV}}$ and these relations are based on the previous knowledge of the process. Then,

$$\delta_{\text{d\_TG}}(k) = 1 \;\Leftrightarrow\; \xi_{\text{d\_TG}}(k) < 0$$
$$\delta_{\text{d\_TV}}(k) = 1 \;\Leftrightarrow\; \xi_{\text{d\_TV}}(k) < 0 \tag{11}$$

Also, as an example of MLD modeling, the mixed integer relation for the first part in Equation (11) is

$$M_{\xi_{\text{d\_TG}}(k)}\delta_{\text{d\_TG}}(k) \leqslant -\xi_{\text{d\_TG}}(k) + M_{\xi_{\text{d\_TG}}(k)}$$
$$(m_{\xi_{\text{d\_TG}}(k)} - \varepsilon_{\xi_{\text{d\_TG}}(k)})\delta_{\text{d\_TG}}(k) \leqslant \xi_{\text{d\_TG}}(k) - \varepsilon_{\xi_{\text{d\_TG}}(k)}$$

where $M_{\xi_{\text{d\_TG}}(k)}$ and $m_{\xi_{\text{d\_TG}}(k)}$ are the maximum and minimum values of $\xi_{\text{d\_TG}}(k)$, respectively. $\varepsilon_{\xi_{\text{d\_TG}}(k)}$ is a small positive scalar.

Equation (11) means when the delay counter reaches 0, then the delay is off. And there is a relation between (11) and 'on' signals:

$$\delta_{\text{on\_TG}}(k) = 1 \;\Leftrightarrow\; \delta_{\text{d\_TG}}(k) = 1 \wedge u_{l1}(k) = 1$$
$$\delta_{\text{on\_TV}}(k) = 1 \;\Leftrightarrow\; \delta_{\text{d\_TV}}(k) = 1 \wedge u_{l2}(k) = 1 \tag{12}$$

The mixed integer representation for the first relation in Equation (12) is:

$$\delta_{\text{d\_TG}}(k) + \delta_{\text{on\_TG}}(k) \leqslant 1$$

$$-u_{l1}(k) + \delta_{\text{on\_TG}}(k) \leqslant 0$$

$$-\delta_{\text{d\_TG}}(k) + u_{l1}(k) - \delta_{\text{on\_TG}}(k) \leqslant 0$$

The other mixed integer relations can also be defined [11]. The CCPP operation modeling has to satisfy a set of constraints that depend on the real operation conditions. Specifically, limits of the flow, temperature and power are added to the MLD system for generating only feasible AHPC outputs.

Using these logical conditions, the adaptive hybrid predictive controller provides two main control actions, $u(k)$:

- On/off signals for gas turbine and steam turbine.
- Proper references for PID controllers during different operation modes of CCPP: start up, normal operation and shut down.

4. MODELING OF AMBIENT TEMPERATURE EFFECT FOR CCPP

Ambient temperature is one of the most uncontrolled and unpredictable variables present in our environment. Nowadays, trustable and accurate prediction models for the ambient temperature do not exist, and this fact makes it almost impossible to apply MPC to any process where ambient temperature affects its behavior.

In the case of a CCPP, the ambient temperature affects mainly the efficiency of the turbines, because it changes the characteristics of the working fluid. The next sections explain the behavior of ambient temperature for the gas and steam turbines and how they are incorporated into the proposed controller design.

Specifically, for the AHPC design, a predictive model for ambient temperature behavior, which strongly affects the power production, is required, and we experimentally corroborate that temperature has a high non-linear behavior. Thus, for its non-linear representation, a fuzzy modeling approach is proposed. Next, a linearized adaptive version of fuzzy models was proposed in order to generate a MLD system that can be incorporated into the proposed AHPC strategy. The main advantage of this approach is to obtain a better approximation of the non-linear behavior of ambient temperature by using adaptive fuzzy models that will be explained in the following sections.

4.1. General behavior of ambient temperature

4.1.1. Gas turbine. The most important problem produced by ambient temperature fluctuations is related to air density changes, i.e. there is less oxygen by volume unit of air and this fact produces a disturbance in the combustion. To avoid this problem, it is necessary to introduce more air and fuel into the combustion chamber. The second most important issue is related to the higher exhaust gas temperature when the ambient temperature increases. Thus, more air flow into the compressor is needed in order to cool down the exhaust gases.

Figure 3 shows the theoretical gas turbine efficiency as a function of the ambient temperature [12]. In this work, three models are used to predict the electrical power and the exhaust gas temperature for a gas turbine. The first model (Model 1) represents the electrical power and the exhaust gas temperature for low ambient temperatures, the second model (Model 2) describes the electrical power and the exhaust gas temperature for medium ambient temperatures, and the last model (Model 3) represents the electrical power and the exhaust gas temperature for high ambient temperatures. The average efficiencies are different for the three models as shown in Figure 3.
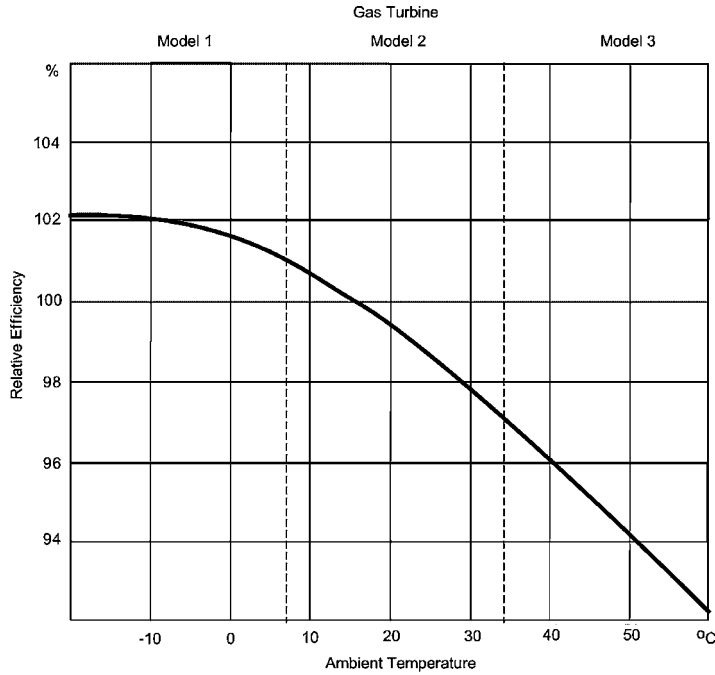
Figure 3. Gas turbine efficiency as a function of the ambient temperature.

4.1.2. Steam turbine. The steam temperature increases its power production at higher ambient temperature. This fact occurs because the exhaust gas temperature increases when the ambient temperature increases.

Figure 4 shows the steam turbine efficiency as a function of the ambient temperature [12]. Following the same procedure that is used for gas turbine, two models were developed. The first model is for low temperatures and the second is for high temperatures.

4.2. Fuzzy modeling

To apply the fuzzy approach into MLD modeling, it is necessary to define the membership functions associated with ambient temperature in order to integrate the three and two models proposed for gas and steam turbines, respectively. Figures 5 and 6 present the membership functions selected for representing the smooth transitions between linear models. The selection of the membership function shape is based on its simplicity and flexibility.

4.2.1. Fuzzy model for gas turbine. Equation (5) for gas power and exhaust gas temperature models are modified in order to include the effect of temperature described in Figure 3:

$$A_{\text{TG1}}(z^{-1})P_{\text{TG}}(k) = \alpha[B_{\text{TG1}}(z^{-1})u_1(k) + B_{\text{TG2}}(z^{-1})u_2(k)]$$
$$A_{\text{TG2}}(z^{-1})T_{\text{TG}}(k) = \beta[B_{\text{TG3}}(z^{-1})u_1(k) + B_{\text{TG4}}(z^{-1})u_2(k)]$$
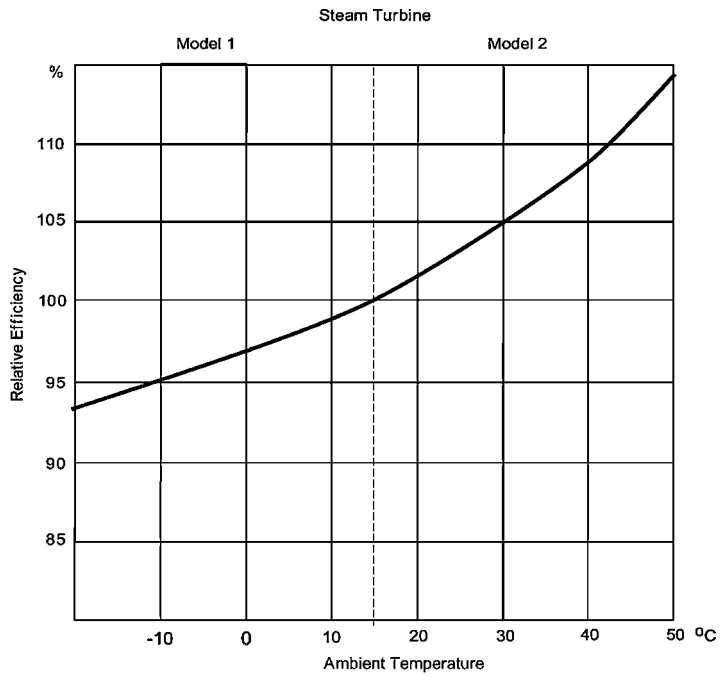
(13)

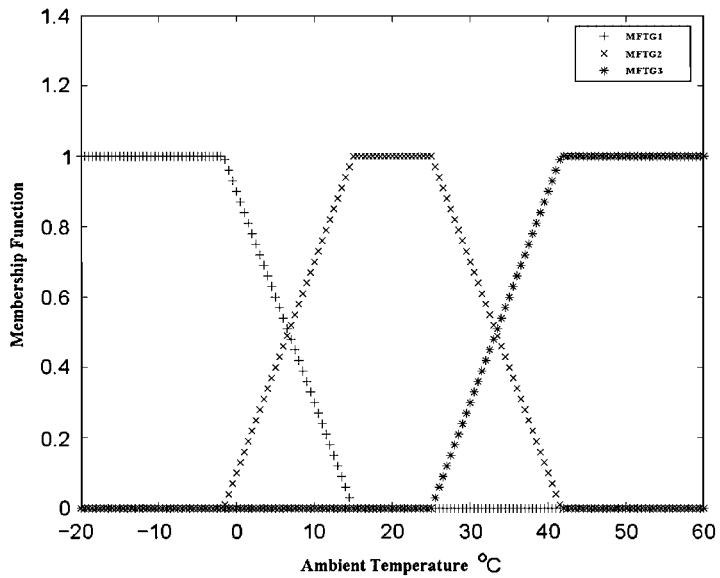Figure 4. Steam turbine efficiency as a function of the ambient temperature.

Figure 5. Membership functions for gas turbine models.

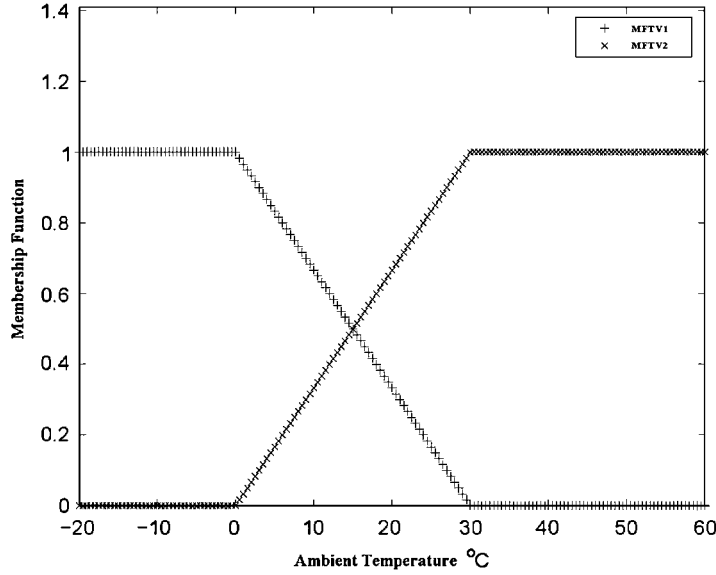Figure 6. Membership functions for steam turbine.

$P_{\mathrm{TG}}(k)$ is the electrical power and $T_{\mathrm{TG}}(k)$ is the exhaust gas temperature, α and β are positive factors that represent the average efficiency of each model described in Figure 3, and therefore, they are associated with three different values depending on the current ambient temperature. Both factors are defined from the thermodynamic properties [12].

In this case, the modeling of the factors is given by the activation degree of each temperature model. Moreover, for every ambient temperature value there is an activation factor for each model. The activation factors α and β are calculated as follows:

$$\alpha = \frac{1.02\mathrm{MF}_{\mathrm{TG1}}(T_{\mathrm{amb}}) + 0.99\mathrm{MF}_{\mathrm{TG2}}(T_{\mathrm{amb}}) + 0.95\mathrm{MF}_{\mathrm{TG3}}(T_{\mathrm{amb}})}{\mathrm{MF}_{\mathrm{TG1}}(T_{\mathrm{amb}}) + \mathrm{MF}_{\mathrm{TG2}}(T_{\mathrm{amb}}) + \mathrm{MF}_{\mathrm{TG3}}(T_{\mathrm{amb}})}$$

$$\beta = \frac{0.98\mathrm{MF}_{\mathrm{TG1}}(T_{\mathrm{amb}}) + 1.01\mathrm{MF}_{\mathrm{TG2}}(T_{\mathrm{amb}}) + 1.05\mathrm{MF}_{\mathrm{TG3}}(T_{\mathrm{amb}})}{\mathrm{MF}_{\mathrm{TG1}}(T_{\mathrm{amb}}) + \mathrm{MF}_{\mathrm{TG2}}(T_{\mathrm{amb}}) + \mathrm{MF}_{\mathrm{TG3}}(T_{\mathrm{amb}})} \tag{14}$$

where $\mathrm{MF}_{\mathrm{TG}i}(T_{\mathrm{amb}})$ is the activation value related to membership function i for gas turbine (Figure 5). This fuzzy approach allows us to include smooth control actions between the model transitions.

4.2.2. Fuzzy modeling for steam turbine. Equation (5) for steam turbine power model is modified in order to include the effect of temperature described in Figure 4

$$A_{\mathrm{TV1}}(z^{-1})P_{\mathrm{TV}}(k) = \gamma B_{\mathrm{TV1}}(z^{-1})u_3(k) \tag{15}$$

where γ is a positive factor that represents the average efficiency of each model described in Figure 4, obtained from the thermodynamic properties [12]. Following the same procedure of

fuzzy modeling described for the gas turbine, the γ factor is given by

$$\gamma = \frac{0.97\text{MF}_{\text{TV1}}(T_{\text{amb}}) + 1.06\text{MF}_{\text{TV2}}(T_{\text{amb}})}{\text{MF}_{\text{TV1}}(T_{\text{amb}}) + \text{MF}_{\text{TV2}}(T_{\text{amb}})} \tag{16}$$

where $\text{MF}_{\text{TV1}}(T_{\text{amb}})$ is the activation value related to membership function i for steam turbine (Figure 6). With this, the resulting prediction model corresponds to an adaptive model as a function of the ambient temperature.

The integration of fuzzy modeling together with the mixed integer representation of the logic sentences gives as a result an adaptive dynamic model that properly fits into the MLD framework.

5. ADAPTIVE HYBRID PREDICTIVE CONTROL ALGORITHM

5.1. Cost function design

The hybrid predictive control design is based on the optimization of the following cost functional [1]:

$$J = C_{\text{dem}} + C_{\text{change}} + C_{\text{fuel}} + C_{\text{start\_up}} + C_{\text{fixed}} - E + C_{\text{start\_up\_gas}} + C_{\text{fixed\_gas}} \tag{17}$$

- C_{dem}: This cost represents a penalty when the electrical power reference and the exhaust gas temperature reference are not fulfilled. This is expressed as follows:

$$C_{\text{dem}} = \sum_{i=1}^{M} p_{\text{dem\_el}}|P_{\text{TV}}(k+i) + P_{\text{TG}}(k+i) - d_{\text{el}}(k+i)|$$
$$+ \sum_{i=1}^{M} p_{\text{dem\_temp}}|T_{\text{TG}}(k+i) - d_{\text{temp}}(k+i)| \tag{18}$$

  where $p_{\text{dem\_el}}$ and $p_{\text{dem\_temp}}$ are positive weights. d_{el} and d_{temp} represent the electrical and the exhaust gas temperature references, respectively. M is the prediction horizon.

- C_{change}: This cost represents a penalty for reducing control action changes over the prediction horizon for obtaining smoother control actions. That is

$$C_{\text{change}} = \sum_{i=1}^{M} p_{\Delta u_1}|u_1(k+i-1) - u_1(k+i-2)|$$
$$+ \sum_{i=1}^{M} p_{\Delta u_2}|u_2(k+i-1) - u_2(k+i-2)|$$
$$+ \sum_{i=1}^{M} p_{\Delta u_3}|u_3(k+i-1) - u_3(k+i-2)| \tag{19}$$

  where $p_{\Delta u_1}$, $p_{\Delta u_2}$ and $p_{\Delta u_3}$ are positive weights.

- C_{fuel}: This term represents the minimization of fuel costs

$$C_{\text{fuel}} = \sum_{i=1}^{M} p_{\text{fuel}}u_1(k+i-1) \tag{20}$$

  where p_{fuel} is a positive weight.

- $C_{\text{start\_up}}$: This term represents the cost when the steam turbine is started up

$$C_{\text{start\_up}} = \sum_{i=1}^{M} p_{\text{start\_up}} \max\{u_2(k+i-1) - u_2(k+i-2), 0\} \tag{21}$$

  where $p_{\text{start\_up}}$ is a positive weight.
- C_{fixed}: This term represents the fixed cost of the steam turbine when it is on

$$C_{\text{fixed}} = \sum_{i=1}^{M} p_{\text{fixed}} u_{l2}(k+i-1) \tag{22}$$

  where p_{fixed} is a positive weight.
- E: This term represents the benefits of selling electrical power

$$E = \sum_{i=1}^{M} p_{\text{el}} \min\{P_{\text{TV}}(k+i) + P_{\text{TG}}(k+i), d_{\text{el}}(k+i)\} \tag{23}$$

  where p_{el} is a positive weight.
- $C_{\text{start\_up\_gas}}$: Analogous to $C_{\text{start\_up}}$ for gas turbine.
- $C_{\text{fixed\_gas}}$: Analogous to C_{fixed} for gas turbine.

Equation (17) uses the absolute value, instead of a traditional square norm used in Equation (4), to simplify the numerical calculations [1]. This permits us to solve the AHPC using mixed integer linear programming and to obtain a reasonable optimum with computational time savings in comparison to the use of square norm which would have to be solved using mixed integer quadratic programming.

The optimization of the cost functional (17), subject to Equation (1), gives the optimal references for the PI controllers of the regulatory level, the on/off signals and delay clock counters for both gas and steam turbines, which correspond to the main optimization variables. These control actions will be a function of the ambient temperature; therefore, the resulting controller will be able to adapt to the ambient conditions. In this case, Equation (1) considers the following items:

- Turbine dynamics (Equation (5)).
- Regulatory control system (Equations (7) and (8)).
- Start-up modes and on/off signals (Equations (9)–(12)).
- Ambient temperature effect (Equations (13)–(16)).

5.2. Solution algorithm

Given that the objective function (17) is non-linear, a non-linear mixed integer optimization problem arises. Its solution allows us to find the optimal references for PID controllers and logical control actions. However, the non-linearities in (17) are special cases that can be recast to a linear function using some particular linear programming methods [11]. Hence, the resulting optimization problem corresponds to a mixed integer linear problem that can be solved using mixed integer linear programming solvers, such as lp_solve of Matlab. Note that by avoiding the use of non-linear optimization functions, such as quadratic functions, the computing time can be made reasonably short allowing a real implementation.

6. SIMULATION RESULTS

In order to test the effectiveness of the proposed AHPC algorithm, it is compared by simulation with a conventional control strategy based on PID controllers and a switching strategy. This simulation test is based on the real data from a thermal power plant of the Central Interconnected System in Chile.

6.1. Plant description

Nehuenco system includes two CCPPs (Nehuenco I and Nehuenco II) and a simple gas turbine (Nehuenco III, open cycle). Nehuenco is located in Quillota, 5th region, Chile, and is a part of the electrical grid of a Central Interconnected System. The maximum electrical power generated by Nehuenco is 852 (MW). In this work, the real data from the CCPP, Nehuenco II, are used (see Figures 7 and 8).

6.2. Evaluation basis

If the ambient temperature is considered as a measured disturbance, then it will be constant within the prediction horizon and will be updated by the receding predictive control strategy.

During the start up, the steam turbine is set up to emulate a hot start up and this is represented by a delay (45 min) between the 'on' command and the current production of electrical power.

The simulation tests are implemented in Matlab version 7.0.1 release 14 running on a Pentium$^{®}$ D CPU 3.20 GHz processor. The sampling time used is 2 min; therefore, the prediction horizon of the controller must be of 23 steps at least in order to include the start up at the right time.

For the strategies comparison, the regulatory control system similar to the one used at Nehuenco power plant is considered, which consists of a switching strategy together with the conventional PID controllers as shown in Figure 1.
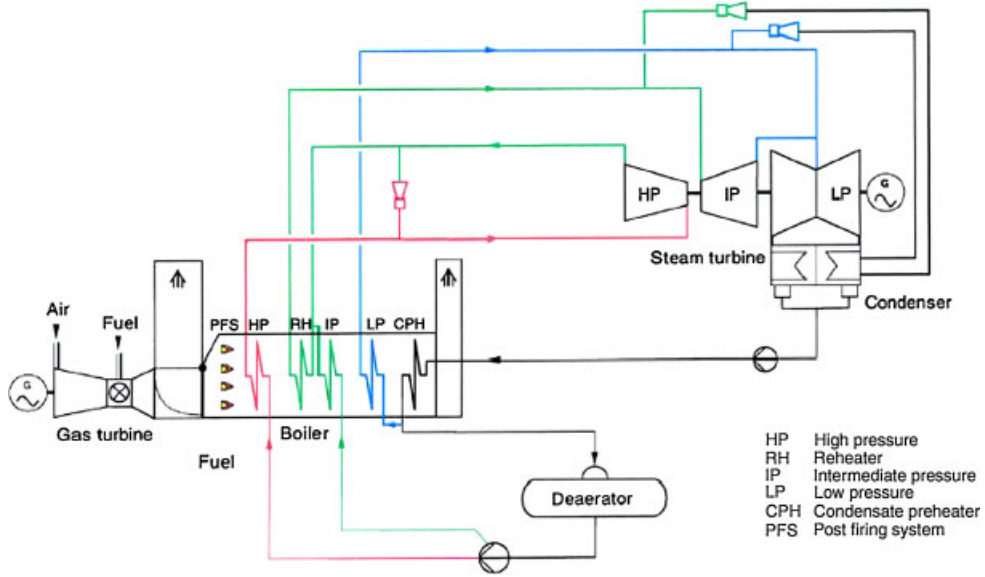

Figure 7. Nehuenco system, Quillota, Chile.

Figure 8. CCPP Nehuenco: simplified layout water/steam cycle.

In order to compare the performance of two regulatory and supervisory control systems, many authors agree on the use of the objective function as an evaluation criterion. However, this comparison is quite unfair, because the supervisory controller, based on predictive control, uses the on-line information provided by the regulatory control system, whereas the regulatory controller does not make use of additional information during its operation.

In order to avoid the situation described previously, the following comparison indexes will be used. The first corresponds to the mean error in electrical power production (MEP) and the second is the average fuel consumption (AFC). Analytically

$$\text{MEP} = \frac{\sum_{i=1}^{T_F} |d_{el}(i) - P_{TV}(i) - P_{TG}(i)|}{T_F}, \quad \text{AFC} = \frac{\sum_{i=1}^{T_F} u_1(i)}{T_F} \tag{24}$$

where T_F is the simulation time.

Equation (25), based on Equation (5), presents the ARX models used for the gas turbine, obtained by using data from the Nehuenco power plant

$$(1 - 0.9363z^{-1})P_{TG}(k) = 5.996u_1(k-1) - 0.11u_2(k-1) + e_1(k)$$
$$(1 - z^{-1})T_{TG}(k) = 0.5845u_1(k-1) - 0.01414u_2(k-1) + e_2(k) \tag{25}$$

where P_{TG} is measured in MW, T_{TG} is measured in °C, and u_1 and u_2 are measured in kg/s.

Equation (26), based on Equation (5), presents the ARX models used for the steam turbine, obtained by using data from the Nehuenco power plant

$$(1 - 0.8871z^{-1})P_{TV}(k) = 0.1586u_3(k-1) + e_3(k) \tag{26}$$

where P_{TV} is measured in MW and u_3 is measured in %.

Table I. Input constraints.

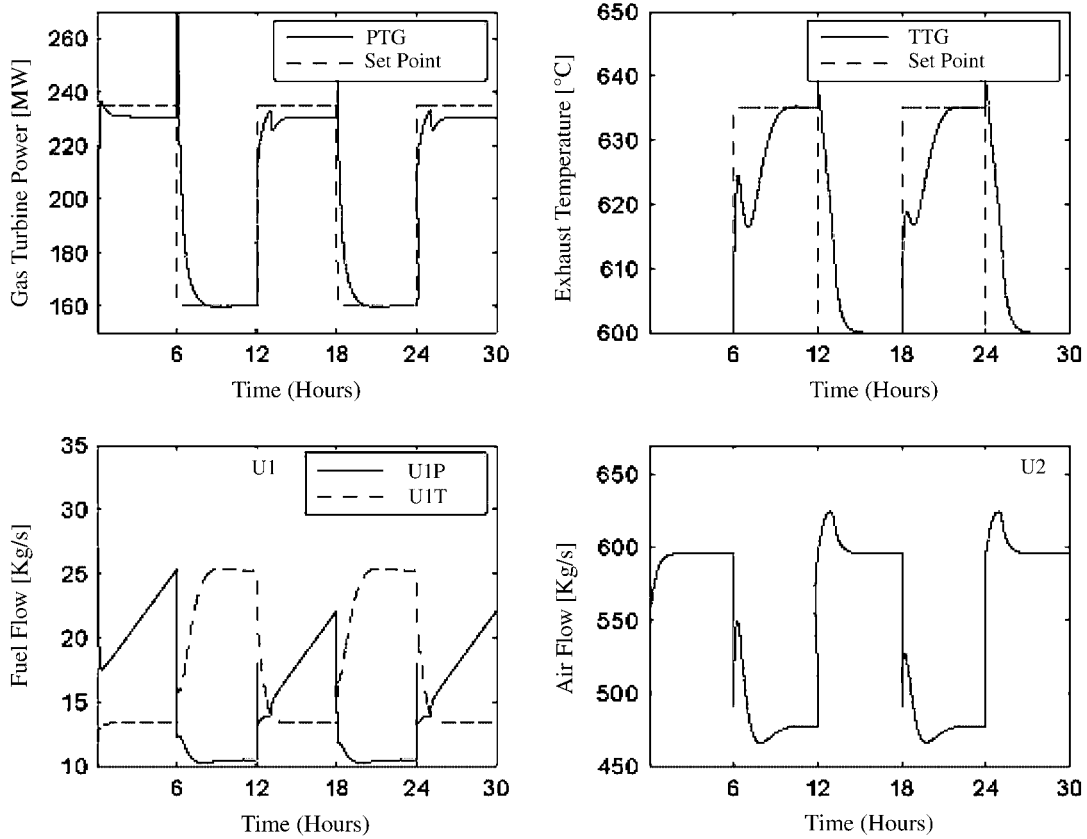| Manipulated variable	Min. value	Max. value
Fuel flow u_1	10 (kg/s)	30 (kg/s)
Air flow u_2	450 (kg/s)	670 (kg/s)
Steam flow u_3	70 (%)	100 (%)

Figure 9. Regulatory PID control strategy for a gas turbine.

The positive factors used are the same as those presented in Equations (14) and (16). The membership functions used in this case are also the ones presented in Figures 5 and 6. Besides, the logic sentences are the same as those presented in Equations (9)–(12). Table I shows the minimum and maximum constraints for the three manipulated variables.

6.3. Results for a gas turbine

Figures 9 and 10 show the responses of the power production and the gas exhaust temperature in the gas turbine for both the regulatory control strategy-based PID controller with switching and
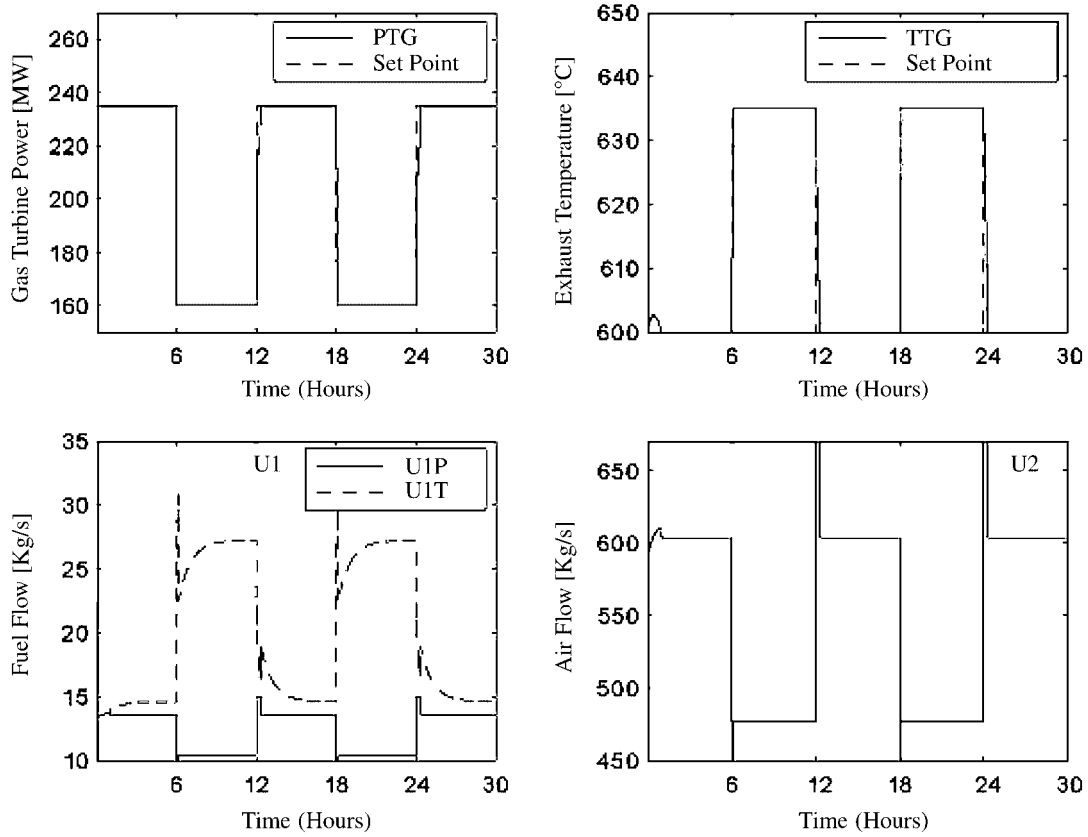
Figure 10. AHPC strategy for a gas turbine.

the proposed AHPC strategy. Also, in these figures, the responses of the fuel and air flows are shown. It can be observed that the output responses improve significantly when using the AHPC strategy. Compared with the regulatory controllers case, the AHPC strategy provides a significant improvement for the system response.

By using the AHPC strategy, the increment in u_1 is minimized in Equation (19) and u_1 is related to u_{1P} and u_{1T} by Equations (6) and (7). Thus, from Figure 10, there is no commutation between u_{1P} and u_{1T} when using AHPC strategy. Analytically, $u_1(k) = u_{1P}$ ($\delta_{PT}(k) = 1$). Moreover, as the AHPC strategy is implemented at a supervisory level, the regulatory switching strategy is compensated. This is corroborated in [4], where the conditions for the equivalence between the supervisory level and regulatory level control strategies based on the same objective function are established.

On the other hand, from Figure 9, there is a continuous commutation between u_{1P} and u_{1T}, due to the fact that the operation of PID controllers is based on that switching strategy.

6.4. Results for the combined cycle power plants

Figures 11 and 12 show the electrical power reference and ambient temperature profile, respectively, for the real power plant in a scale version of the real data. In the electrical power reference (see
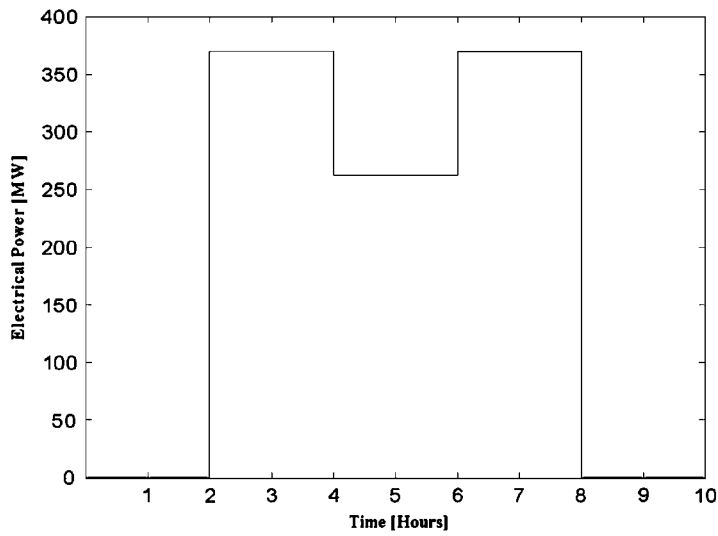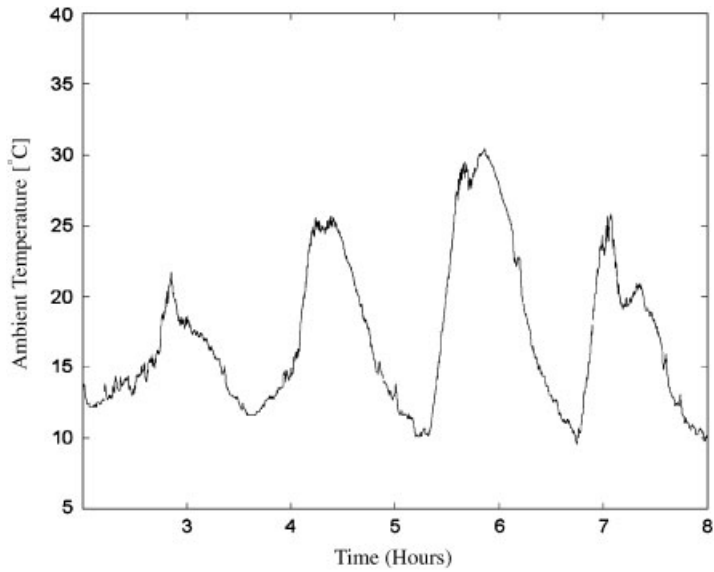
Figure 11. Electrical power reference.

Figure 12. Ambient temperature profile.

Figure 11) three different stages of the power plant are shown: start up, normal operation and shut down. The ambient temperature profile (see Figure 12) used corresponds to spring; therefore, the maximum and minimum are according to the characteristics of that season.

Figure 13 shows the responses of the electrical power and the exhaust gas temperature obtained from the proposed hybrid predictive controller. Also, Figure 14 shows the following control
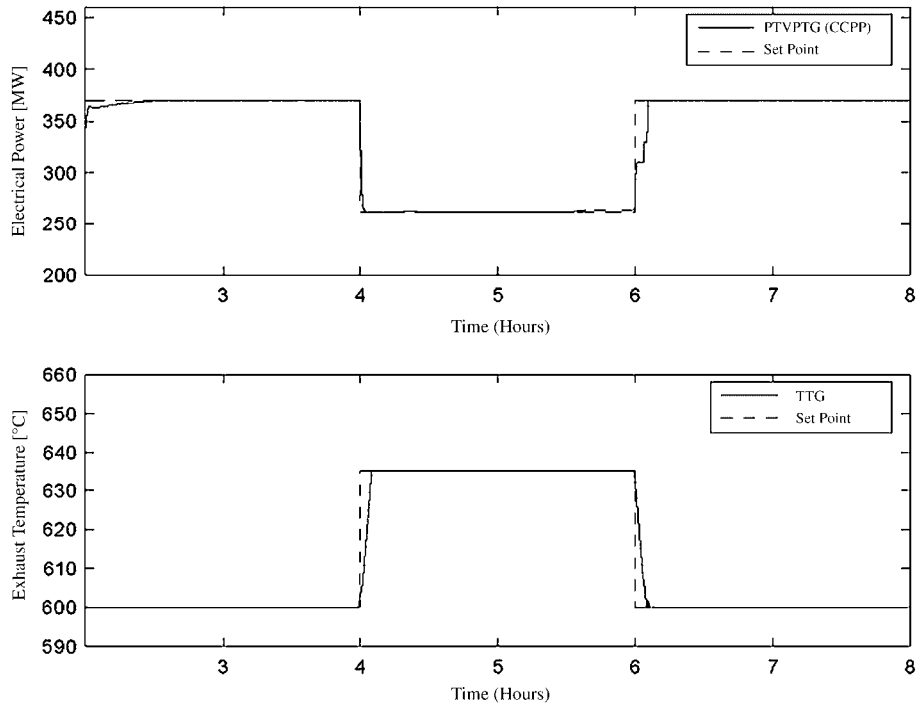
Figure 13. AHPC strategy. Power output and gas turbine exhaust temperature.

actions: fuel flow, air flow and steam flow. The gas turbine exhaust temperature reference is related to the electrical power reference as shown in Figure 13.

As shown in Figure 13, we can appreciate good tracking capacities and short settling times. As seen in Figure 14, the switching of the PID controllers, which regulate the fuel flow, has been almost eliminated. This fact shows that it is possible to control the exhaust gas temperature and the electrical power, without using a switching strategy.

For the control system, a critical situation is observed around instant time (6 h), at which the ambient temperature has a peak (see Figure 12) and the plant increases its power generation (see Figure 11). In this case, from Figure 14, the apparent switching that occurred at hour 6 is not real: instead, the controller takes u_{1T} as a dynamic upper boundary for u_{1P}; therefore, u_{1P} never exceeds u_{1T}. This behavior is quite interesting because the optimization algorithm decided to reduce the switching of controllers, and therefore, minimize the control energy. The air flow is also regulated in the gas turbine, in order to maintain a good air/flow ratio, which assures a good combustion and consequently low NO_x emissions.

Besides, at the sixth hour the exhaust gas temperature tends to be higher than the normal average and at the same time, the electrical power reference increases (see Figure 11) and with this the consumption of fuel, which also increases the exhaust gas temperature. As shown in Figure 13, for this situation, the adaptive hybrid predictive controller prefers to maintain the exhaust gas temperature at a safe level and once this has been achieved, it proceeds to take the electrical power to the desired level. This behavior is suitable for maintaining the lifetime of the gas turbine.
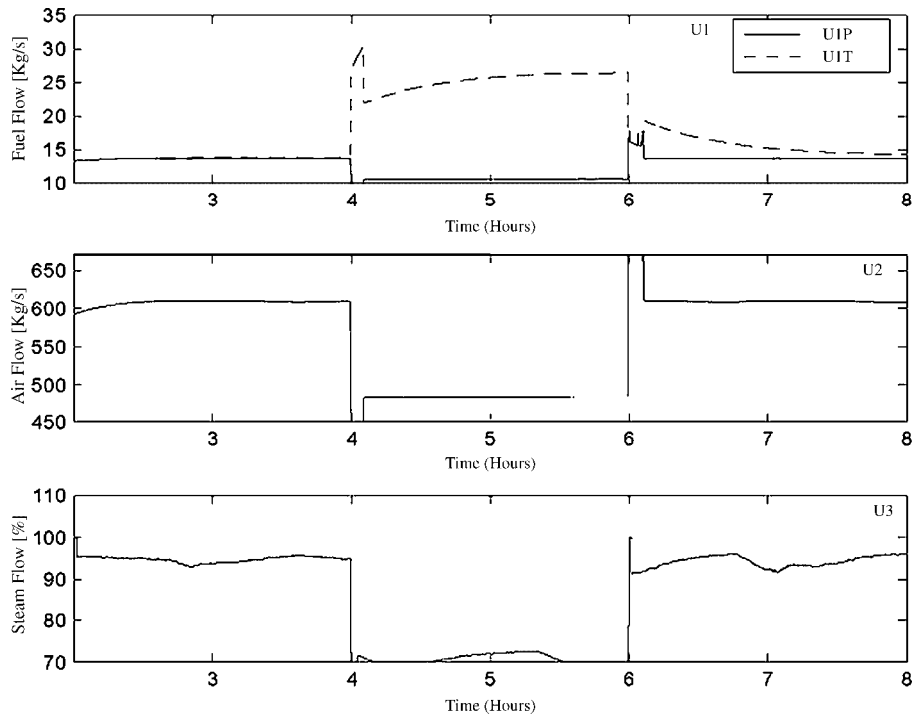
Figure 14. AHPC strategy. Manipulated variables of CCPP.

In the case of the steam turbine, the steam flow is modified for minimizing the ambient temperature effect over the electrical power produced. Note that when the ambient temperature rises, the steam flow falls, because at higher ambient temperatures, less steam flow is needed in order to produce the same electrical power. In fact, the limit constraints of the manipulated variables are satisfied as well, in particular, between the 4th and 6th hours.

The ambient temperature effect on the control variables is significantly reduced due to the appropriate selection of the corresponding control actions, such as air flow, fuel flow and steam flow, as shown in Figure 14.

If the ambient temperature changes between 10 and 30°C in this experiment, the steam turbine is more affected than the gas turbine; this can be clearly seen in Figures 3, 4 and 12, where model 2 of the gas turbine is mainly selected, but both models (1 and 2) of the steam turbine are also selected.

Figure 15 shows the results of on/off commands (superposed) for gas and steam turbines using the adaptive hybrid predictive controller. Because of AHPC algorithm, both turbines are started up at time 1:15 and seen in Figure 11, the actual power production of both synchronized turbines starts at 2:00 and, therefore, the constraint defined in Section 6.2 given by the delay of 45 min is satisfied. The constraint corresponds to the 'hot start' condition of the steam turbine (Equation (10)).

Table II presents a comparison between the AHPC strategy and a conventional PID strategy which is the current control algorithm used in Nehuenco II. The AFC shows a 3% of savings in comparison with the regulatory controller.
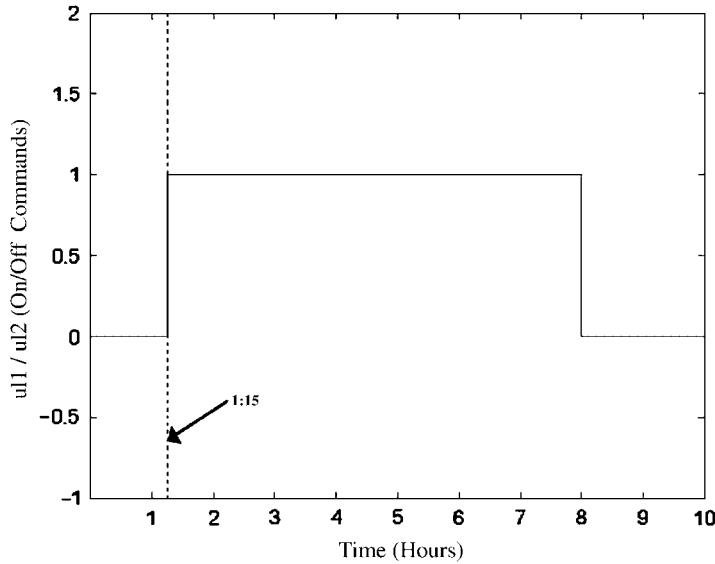
Figure 15. On/off signals.

Table II. Comparison indexes.

Control strategy	MEP (MW)	AFC (kg/s)
Regulatory PID control strategy	0.63152	12.8025
AHPC strategy	0.60041	12.4023

7. CONCLUSIONS

This paper has presented the complete design of an adaptive hybrid predictive controller for a real CCPP. The plant has been modeled as a hybrid system, which includes operational modes: start up, normal operation, and shut down. The ambient temperature effect has been represented using fuzzy models, which allows us to obtain smoother control actions and to include these fuzzy models along with MLD schemes. The proposed design is tested in a model of a real CCPP, Nehuenco II, obtaining a better performance in comparison to the conventional control system, resulting in a 3% saving of fuel consumption and better tracking capacities. By using the proposed AHPC, we can observe that it is possible to control the exhaust gas temperature and the electrical power production without the need of using the traditional switching strategy.

The future work considers including a detailed representation of the start-up mode of the CCPP given by the thermal stress modeling. The frequency controller of turbines will also be included. We hope to prove that the AHPC minimizes the start-up time and reacts adequately under electrical grid frequency disturbances.

REFERENCES

1. Ferrari-Trecate G, Gallestey E, Letizia P, Speticato M, Morari M. Modeling and control of co-generation power plants: a hybrid system approach. *IEEE Transactions on Control Systems Technology* 2004; **12**(5):694–705.
2. Arroyo JM, Conejo AJ. Optimal response of a thermal unit to an electricity spot market. *IEEE Transactions on Power Systems* 2000; **15**(3):1098–1104.
3. Arroyo JM, Conejo AJ. Modeling start up and shut down power trajectories of thermal units. *IEEE Transactions on Power Systems* 2004; **19**(3):1562–1568.
4. Sáez D, Cipriano A, Ordys A. *Optimization of Industrial Processes at Supervisory Level*: Application to Control of Thermal Power Plants. Series Advances in Industrial Control. Springer: Berlin, 2002.
5. Sáez D, Ordys A, Grimble M. Design of a supervisory predictive controller and its applications to thermal power plants. *Optimal Control Applications and Methods* 2005; **26**(4):169–198.
6. Al Seyab RK, Cao Y. Nonlinear model predictive control for the Alstom gasifier. *Proceedings of the 16th IFAC World Congress*, Prague, Czech Republic, Paper Mo-R06-TO/6, July 2005.
7. Camacho E, Bordons C. *Model Predictive Control*. Springer: Berlin, 1999.
8. Bemporad A, Morari M. Control of systems integrating logic, dynamics and constraints. *Automatica* 1999; **35**:407–427.
9. Takagi T, Sugeno M. Fuzzy identification of systems and its application to modeling and control. *IEEE Transactions on Systems*, *Man and Cybernetics* 1985; **SMC-15**:116–132.
10. Ordys A, Pike A, Johnson M, Katebi R, Grimble M. *Modeling and Simulation of Power Generation Plants*. Series Advances in Industrial Control. Springer: Berlin, 1994.
11. Mignone D. The really big collection of logic propositions and linear inequalities. *Technical Report*, *AUT01-11*, 2002.
12. Kehlhofer R. *Combined Cycle Gas & Steam Turbine Power Plants*. PennWell Corp.: Oklahoma, U.S.A., 1999.